MODELING THE EFFECTS OF LASER-BEAM SMOOTHING ON FILAMENTATION AND STIMULATED BRILLOUIN BACKSCATTERING

R. L. Berger *C. W. Still* *S. N. Dixit*
T. B. Kaiser *A. B. Langdon* *D. I. Eimerl*
B. F. Lasinski *E. A. Williams* *D. Pennington*

Using the three-dimensional code (F3D), we compute the filamentation and backscattering of laser light. The results show that filamentation can be controlled and stimulated Brillouin backscattering (SBBS) can be reduced by using random phase plates (RPP)[1] and small *f*-numbers or smoothing by spectral dispersion (SSD)[2] with large bandwidth. An interesting result is that, for uniform plasmas, the SBBS amplification takes place over several laser axial coherence lengths (coherence length ≈ speckle length ≈ $8f^2\lambda_0$, where λ_0 is laser wavelength).

Introduction

Controlling stimulated Brillouin scattering (SBS) and filamentation are essential to the success of laser fusion because together they affect the amount and location of laser energy delivered to the hohlraum wall for indirect drive and to the absorption region for direct drive. Filamentation and self-focusing occur when a density depression is produced by the nonuniform light intensity through ponderomotive and thermal pressures. Light refracts toward lower densities, and the light intensity increases until diffractive losses limit the lateral dimension of the nonuniformity. The incident laser beam has strong intensity nonuniformities, so that even modest filamentation gain may be unacceptable. Moreover, filamentation is the suspected reason that significant levels of SBS and stimulated Raman scattering (SRS) are observed even when calculated gain exponents are modest ($G < 5$). Because the length of laser beam hotspots is much larger than the width (ratio of length to width is ~8*f*), backscattering is expected to be more important than sidescattering. Without hotspots, the gain rate and the growth rate of backscattering in a uniform plasma are not much different from those of sidescattering. For example, if the acoustic wave is weakly damped, the backscattering Brillouin growth rate is only $2^{1/4}$ times the sidescatter rate. Laser-beam smoothing schemes such as SSD and induced spatial incoherence (ISI)[3] illuminate the target at best focus where the laser spot is comprised of a large number of diffraction-limited hotspots. Therefore, understanding the laser–plasma interaction with hotspots is essential. We illustrate the effects of filamentation in Figure 1 where surfaces that enclose volumes in which laser intensity is higher than five times the average intensity are shown. Figure 1(a) shows the surfaces before any self-focusing has developed. Figure 1(b) shows the surfaces after the filaments have developed. There is an obvious increase in the number of high-intensity regions.

In previous reports[4,5] we presented the equations, the approximations and their justification, the numerical techniques, and some results obtained with the F3D code. This code does three-dimensional (3-D) calculations of the propagation of laser beams in which the laser light self consistently filaments and Brillouin backscatters.

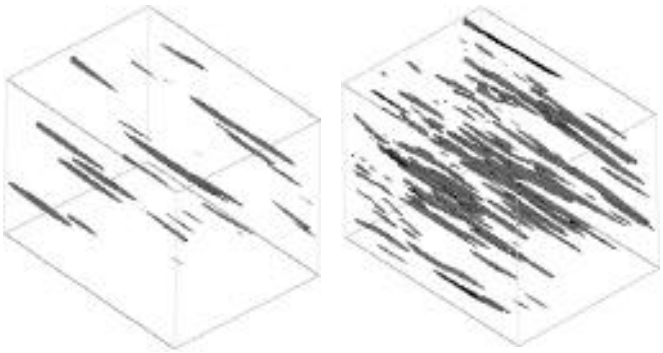

FIGURE 1. Three-dimensional surfaces within which the laser intensity is greater than five times average (a) before filamentation and (b) after filamentation. (50-01-0895-1872pb01)

Here, we review laser-beam smoothing techniques and present the effects of temporal beam incoherence on filamentation and SBBS. Because filamentation and backscattering are the dominant interactions in the problems we consider, we can separate the light wave into a nearly forward- and nearly backward-moving wave, each treated within the paraxial approximation. Similarly, we can separate the acoustic wave response into long-wavelength modes, driven by filamentation or forward scattering, and short-wavelength modes, driven by backscattering. This separation allows us to consider fairly large regions of underdense plasma, containing many hotspots, because the spatial resolution necessary with this scheme is much less than in treatments that solve the full wave equation.[6] This allows us to consider the influence of SSD and other temporal beam-smoothing techniques on filamentation and SBBS.

Effect of Laser-Beam Smoothing on Filamentation

In the focal spot of a laser beam focused with an RPP, the laser intensity is highly modulated with a $\mathrm{sinc}^2(X)$ $\mathrm{sinc}^2(Y)$ envelope; here $X = \pi x d_x / f_1 \lambda_0$, $Y = \pi y d_y / f_1 \lambda_0$, where d_x and d_y are the RPP element sizes in the transverse x and y directions, f_1 is the lens focal length, and λ_0 is the laser wavelength. On the smaller scale of the diffraction-limited spot for the full lens aperture D, there are hotspots (speckles) with a distribution of intensities up to N times the average, where $N = \mathrm{D}/d_x$ for square RPP array. The laser beam can focus on the scale of the laser spot $f_1\lambda_0/d_x$ (whole-beam self-focusing), on the scale of the speckles $f\lambda_0 = f_1\lambda_0/\mathrm{D}$ (filamentation), and on scales between these limits (filamentation). Laser-beam smoothing is primarily intended to suppress the filamentation process, which occurs on a much shorter time scale than whole-beam effects. Here, we consider the evolution of filamentation for a representative portion of the beam because simulation of the whole beam, including the small-scale structure, cannot be done for realistic laser beam diameters (>1000λ_0). In previous reports[4,5,7] we showed that filamentation is stable if the length of the speckle l_s is shorter than the minimum spatial gain length l_g, where

$$l_g^{-1} = K_{\max} = 0.125 \frac{v_0^2}{v_e^2} \frac{n_e}{n_c} \frac{\omega_0}{c} \quad . \tag{1}$$

with $\omega_0/c = 2\pi/\lambda_0$. K is the filamentation spatial gain rate, c is the speed of light, n_e is the electron density, n_c is the critical density, $v_0 = eE/m_e\omega_0$ is the jitter velocity of an electron in the laser electric field, and v_e is the electron thermal velocity. An equivalent statement is that stability against filamentation requires that the gain exponent for filamentation in a plasma one speckle length long be less than unity.

When this criterion is not satisfied, temporal smoothing is required to stabilize filamentation. For example, we have $l_g < l_s$ for parameters appropriate to the National Ignition Facility (NIF) design[8,9] (e.g., for $f/8$, $0.1n_c$, electron temperature $T_e = 3$ keV, intensity $I = 2\times10^{15}$ W/cm^2, $\lambda_0 = 0.351$ μm, we have $l_g = 0.8l_s$ and $l_s = 180$ μm). For an ISI or SSD scheme, the speckles dissolve and reform in different locations on the time scale of the laser coherence time $\Delta\omega^{-1}$. Conversely, the intensity in a speckle increases at the rate Kc; thus, we estimate that SSD or ISI will stabilize filamentation if $\Delta\omega > Kc$. The criterion $\Delta\omega > Kc$ corresponds to

$$\frac{\Delta\omega}{\omega_0} = \frac{\Delta\lambda}{\lambda_0} > 4.6\times10^{-4} \frac{n_e}{10^{21}\,\mathrm{cm}^{-3}} \frac{I}{2\times10^{15}\,\mathrm{W/cm}^2} \times \frac{3\,\mathrm{keV}}{T_e} \left(\frac{\lambda_0}{0.351\,\mu\mathrm{m}}\right)^4 \quad . \tag{2}$$

Figures 2 and 3 show two measures of the effect of SSD bandwidth on filamentation. The simulation dimensions were typically 160 wavelengths along x and y and 530 wavelengths along z, the direction of propagation. Figure 2(a) shows the fraction, F, of laser beam energy above five times the average intensity as a function of laser bandwidth for a simulation case that was strongly unstable without SSD (i.e., for the NIF parameters listed previously but with laser intensity 4×10^{15} W/cm^2). This fraction F varies with z from the initial value of ~4% at $z = 0$ to a maximum value followed in general by a decrease at larger z as the beam breaks up. The fraction displayed is the maximum value. For sufficient bandwidth, this fraction is reduced to that for an RPP beam in vacuum. Figure 2(a) also shows the extent to which four-color illumination (described below) combined with SSD inhibits filamentation.

Figure 2(b) compares the distribution of intensities in several cases with that for an RPP beam in vacuum.[10] The distributions plotted are for the simulation region in which the fraction shown in Fig. 2(a) is largest. In the no-SSD case (3120) beam energy is transferred to very high intensity at the expense of energy between 1–5 times the average. Note that this intensity-weighted distribution peaks at 2–3 I_0 in all cases, but the total energy is constant except for the loss to collisional absorption; thus the initial distribution has the most energy. The addition of a small bandwidth, $\Delta\omega/\omega_0 = 0.025\%$ (case 3123), is not very effective, but it does reduce the population of the most intense hotspots. In the large-bandwidth case (3205), $\Delta\omega/\omega_0 = 0.15\%$, very little energy is transferred to intensities $I > 10I_0$. In fact between 4 and 10 I_0, this distribution has less energy than the initial RPP case. The fraction of beam energy at high intensity peaks near the region where the first foci occur and

relaxes to a less energetic distribution at greater distances. However, this relaxation comes at the expense of increased beam divergence as the speckles get narrower and shorter.

Figure 3 shows contour plots of the total laser energy in transverse Fourier modes at a given z vs k_x and k_y for the small and large SSD bandwidths. The incident wave has no energy for values of $|k_x| > k_0/2f = 0.0625k_0$ or $|k_y| > k_0/2f$ for an $f/8$ lens. Filamentation breaks the beam into smaller-scale hotspots, which appear in this type of plot as an increase in the energy at higher $k_\perp$. Thus in Fig. 3(a), the filamented distribution shows a significant amount of energy outside the incident beam cutoff, whereas the SSD-stabilized case in Fig. 3(b) shows a small amount of energy at these $k_\perp$. These plots also represent the amount of energy outside a given angle in the near field (lens image plane) vs the angle. Such measurements are being made in Nova experiments.[11]

For 3ω illumination, the bandwidth required to stabilize filamentation at intensities in excess of 2×10^{15} W/cm^2 cannot be used because the tripling efficiency is too low for bandwidths $\Delta\lambda/\lambda_0 \geq 3 \times 10^{-4}$. A different temporal scheme was proposed[12] wherein four narrow-band laser beams with slightly different wavelengths are focused using different quadrants of the lens to overlap in the target plane. The interference pattern (the speckles) then moves periodically in time,

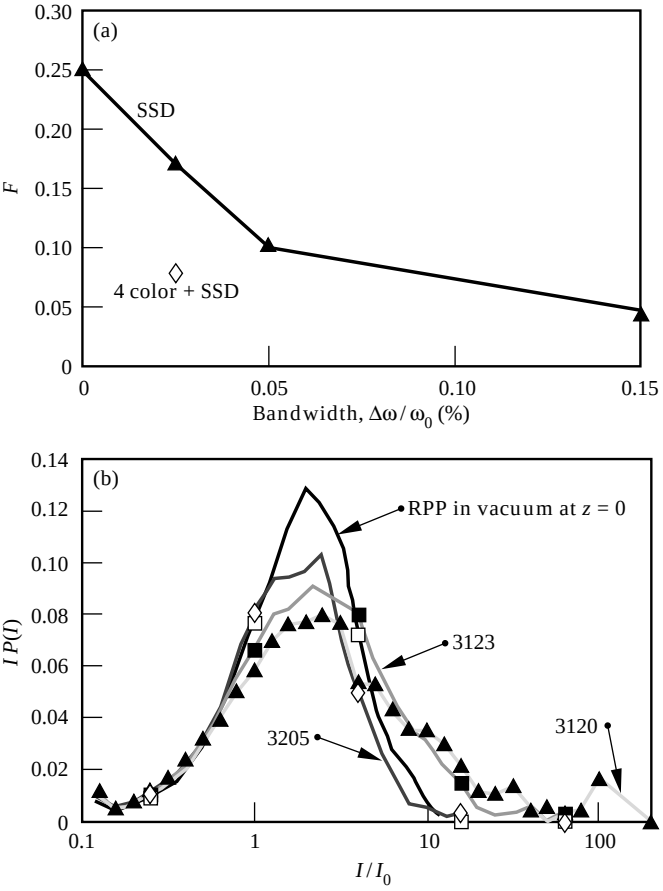

FIGURE 2. (a) Fraction F of the laser beam energy above five times the average intensity as a function of the SSD bandwidth for an $f/8$, $I_0 = 4 \times 10^{15}$ W/cm^2 laser beam. Also shown is one case combining four-color illumination with SSD. (b) The intensity weighted distribution. For the initial distribution at $z = 0$, the integral of the distribution is unity (i.e., the average is I_0), but it is less than unity for $z > 0$ because of collisional absorption. (50-01-0895-1882pb01)

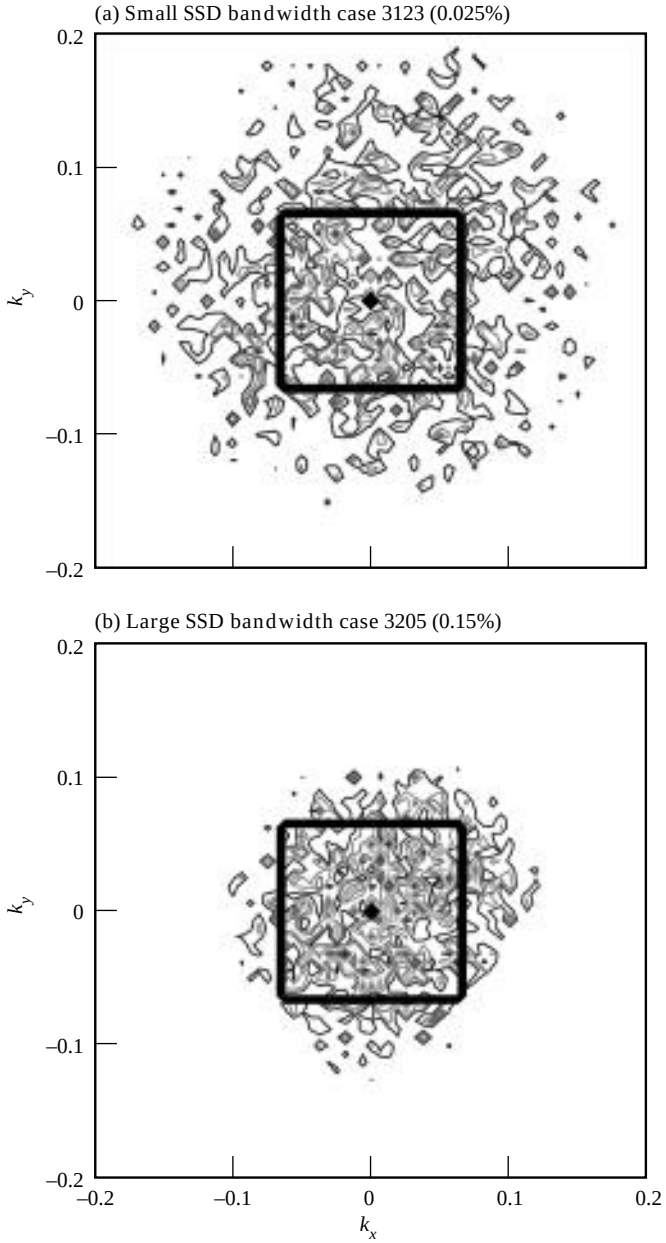

FIGURE 3. Fourier components of the laser beam energy with average $I_0 = 4 \times 10^{15}$ W/cm^2 for the incident beam at $z = 0$, and after propagating $500\lambda_0$ for (a) an SSD bandwidth of 0.025% and (b) an SSD bandwidth of 0.15%. The incident laser beam energy is uniformly distributed over perpendicular wavelengths that fit within an $f/8$ square aperture lens. (50-01-0895-1874pb01)

not randomly as in an SSD or ISI scheme. If the frequency separation between adjacent lines is $\delta\omega$, the time t_r for the speckle pattern to repeat is $t_r = 2\pi/\delta\omega$. The time-averaged speckle pattern is not smoothed because the $f/16$ speckles produced by each quadrant of the lens are unaffected. This four-color scheme[13] stabilizes filaments from the $f/8$ structure but unfortunately does not stop filaments from forming due to the remaining static $f/16$ speckles. Nonetheless, with four-color illumination, it is the intensity per quadrant that counts, and the spatial growth rate is decreased by a factor of four. However, since the speckle length has effectively increased by a factor of four, the net effect in plasmas longer than an $f/16$ speckle is to increase the distance over which the beam propagates before breaking up. Filamentation stability can be recovered with the introduction of SSD with a bandwidth of 0.025% (if used in conjunction with four-color illumination) because the $f/16$ speckles (and even longer wavelength structures) are now temporally smoothed. Equation (2) can be used to estimate the minimum four-color separation needed with $\delta\omega = \Delta\omega_{min}/3$ provided $\Delta\omega_{SSD} > \Delta\omega_{min}/4$. For the nominal parameters of the NIF, $\Delta\lambda_{min} \approx 0.5$ nm before frequency tripling ($\Delta\lambda_{min} = 0.17$ nm at 0.351 μm), so an SSD bandwidth $\Delta\lambda_{SSD} = 0.25$ nm is twice what is estimated as necessary.

This work only addresses the stability of the speckles on the small scale. Focusing can also occur on the larger scale of the whole beam. Four-color illumination and SSD will have little effect on that process. Dixit has pointed out[14] that the grating dispersion need only be large enough to displace the hotspots by a speckle width to temporally smooth the intensity pattern, at least in a model that neglects phase errors and lens aberrations. We surmise that, in the more general case, laser beams may filament on scales intermediate between the speckle size and the whole beam, and larger grating dispersion may help in this case.

Effect of Laser-Beam Smoothing on Stimulated Brillouin Backscattering

The spatial structure of the laser beam on the scale of a speckle and temporal smoothing of the hotspots have an effect on the spatial and temporal growth of SBBS. For SBS, there is an additional effect possible that survives in a 1-D treatment even if the hotspots are stationary, namely that the convective or early-time growth rate of SBS is reduced if $\gamma_0 < \Delta\omega$ and $\Delta\omega > \mathrm{Max}(\upsilon_a, \upsilon)$, where υ_a and υ are the damping rates of the acoustic and light wave, respectively. The weakly coupled SBBS growth rate γ_0, given by

$$\frac{\gamma_0}{\omega_0} = \frac{1}{4}\frac{v_0}{v_e}\frac{\omega_{pe}}{\omega_0}\left(\frac{\omega_a}{\omega_0}\right)^{1/2}$$

$$\cong 8\times10^{-4}\left(\frac{I}{2\times10^{15}\,\mathrm{W/cm^2}}\right)^{1/2}\left(\frac{\lambda_0}{0.351\mu\mathrm{m}}\right)^2$$

$$\left(\frac{n_e}{10^{21}\mathrm{cm^{-3}}}\right)^{1/2}\times\left(\frac{3\,\mathrm{keV}}{T_e}\right)^{1/4}\left(\frac{Z}{A}\right)^{1/4}, \qquad (3)$$

is in general larger than the laser bandwidth, especially in the hotspots. For multispecies plasmas, $Z/A \to \left(Z_j^2/A_j\right)/\left(Z_j\right)$, where the averages of the charge states Z and atomic numbers A are taken over the ion species j. This expression for γ_0 applies if $ZT_e/T_i \geq 3$ for all species in multispecies plasma and $k\lambda_{De} < 1$ where λ_{De} is the electron Debye length. If the fluid approximation for either species does not apply, the frequency and damping characteristics of the acoustic mode are significantly modified.[15] For narrowband four-color illumination, $\Delta\omega$ can be larger than γ_0, and a reduction in SBS without beam smoothing might occur. However, in our simulations, since four-color illumination always causes the hotspots to move, the pure bandwidth effect on SBS has not been studied. In summary, we expect no effect on SBS from bandwidth without smoothing (i.e., there is no dispersion and the speckles are stationary); none is observed in our $\gamma_0 < \Delta\omega$ simulations.

As discussed in the previous section, the laser speckle size in the focal plane region affects the stability of the laser light against filamentation. Our initial expectation was that the SBBS would occur independently in each speckle and thus be very sensitive to the laser *f*-number,[16] but our simulations in uniform plasmas showed that the spatial amplification occurred over many speckle lengths. The primary determinant of the reflectivity, when the laser intensity is below the absolute growth threshold, is the convective gain exponent

$$G = \frac{1}{8}\frac{v_0^2}{v_e^2}\frac{n_e}{n_c}\frac{\omega_a}{\upsilon_a}\frac{\omega_0 L}{c}, \qquad (4)$$

where L is the axial system length. Note that the spatial gain rate for SBBS is higher than that for filamentation by the ratio ω_a/υ_a. This fact has consequences in the simulations, which we discuss later.

Figure 4 shows the SBBS reflectivities from our simulations without temporal smoothing as a function of G for $f/8$ and $f/4$ laser illumination. The $f/8$ reflectivity is systematically higher than that for $f/4$ for the same plasma conditions and laser intensity. The difference is much less than a single-hotspot model would predict because, then, the gain exponent per speckle would be

the figure of merit. For example, for a single-hotspot model, the $f/4$ reflectivity with a gain exponent of 20 should be four times the $f/8$ value with a gain exponent of 5 if all other factors were constant. The factor of four comes from the fact that the number of hotspots per axial length is larger for $f/4$. That clearly is not the result of the simulations.

Another measure of *f*-number effects is the gain exponent above which significant reflectivity occurs. Figure 4 indicates that this gain exponent is ~4 for $f/8$ and ~6 for $f/4$; these exponents are in the ratio 1.5, not $(8/4)^2 = 4$, as would be expected from a single-hotspot model.

Some of the difference between the $f/8$ and $f/4$ simulations may be the result of some filamentation in the $f/8$ case since, for intensities higher than $\sim 2 \times 10^{15}$ W/cm^2, the $f/8$ laser light is unstable against filamentation. Simulations for $f/8$ in which the light refraction was neglected (but the hotspots remained) showed about a factor of two decrease in reflectivity at $G = 12$. Another reason may be incomplete phase conjugation, as discussed below.

We have concentrated on modeling laser and plasma processes relevant to the NIF and to current Nova experiments. For these parameters, filamentation in fact has less influence on the SBBS results than we expected. First, with average laser intensities less than 5×10^{15} W/cm^2, $f/4$ speckles are stable against filamentation. With $f/8$ focusing, filamentation is important above 2×10^{15} W/cm^2, but then the SBS gain is so high in our uniform plasma simulations (for the range of damping rates used) that the laser intensity becomes depleted before filaments *fully* develop. That is, as the hotspots start to focus, the laser intensity increases,

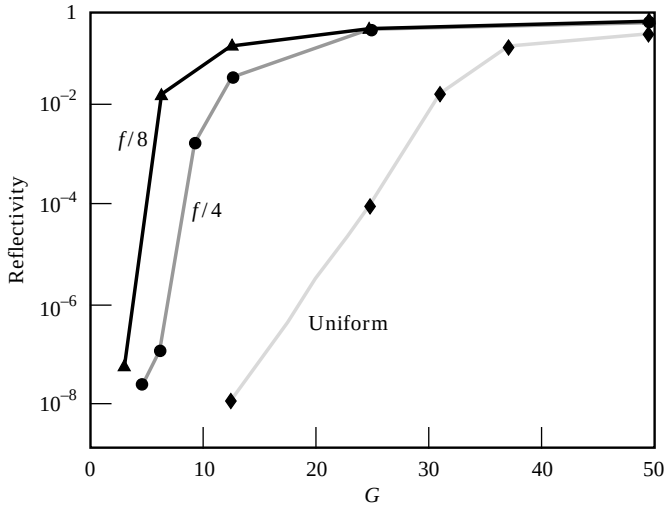

FIGURE 4. SBS reflectivity vs 1-D gain exponent for temporally unsmoothed $f/8$, $f/4$, and uniform laser beams. (50-01-0895-1876pb01)

which increases the growth rate of SBBS. Then the backward-moving light robs power from the forward-moving light, making the rate of focusing less than it would be without SBBS. If the gains were lower, filamentation would cause more of a difference between $f/4$ and $f/8$ reflectivities. In reality, SBBS may saturate before the laser intensity is depleted because of *nonlinear limits* on the SBBS growth;[17] this is the focus of our current research.[18]

A heuristic explanation for the weak dependence of SBBS on the *f*-number involves the notion of phase conjugation.[19] The pattern of speckles at any $z > 0$ for the incident laser light is determined by the amplitude and phase of the transverse Fourier components at $z = 0$. A light wave of nearly the same frequency propagating in the backward direction, e.g., an SBBS wave, would have the same pattern of speckles between zero and z if its components had the same relative amplitude but the conjugate phase of the incident light at z. (Of course, this is only true if filamentation, sidescattering, or other nonlinear processes do not alter the propagation substantially.) From all the light waves that the plasma produces as a result of collisional emission or Thomson scattering, those whose phase and Fourier components match those of the incident light will be amplified most because, over many speckle lengths, their hotspot patterns overlap that of the incident light. As yet, we do not have a statistical measure of the degree of phase conjugation; however, we have examined sequences of 2-D x–y plots comparing the incident-beam and reflected-light hotspots at several planes in z separated by more than a speckle length. The reflected-light hotspots are always associated with a laser-beam hotspot.

Now, consider a plasma one $f/8$ speckle length long. For $f/8$ illumination, the SBBS will grow in hotspots of about the same length as the plasma and will experience a gain in excess of the uniform-intensity gain. The $f/4$ SBBS will initially grow in the backward direction in a hotspot of 0.25 the plasma length, and, if phase conjugation does not occur, it will grow at a reduced rate once the waves leave their hotspots. However, because of the collective effect of phase conjugation, the backward light wave's hotspots overlap those of the incident laser wave and continue to drive ion acoustic waves efficiently through the ponderomotive force (proportional to the product of the light wave amplitudes). Thus the SBBS grows in $f/4$ hotspots almost as effectively as in the $f/8$ hotspots.

As discussed earlier, the laser bandwidth available at 0.35 μm on Nova is too low to reduce the amplification or growth rate directly . However, given that the SBBS grows in hotspots and takes many growth times to reach saturation, SSD or an equivalent beam-smoothing technique may be effective in reducing the reflectivity because the hotspots are no longer stationary. In addi-

tion, if the gain occurs over an extended region of plasma, the phase coherence of the incident wave with the reflected wave will be reduced with the reduction in reflectivity.

Figure 5 shows the reflectivity as a function of G for $f/4$ illumination with and without temporal beam smoothing. The results for one-color, four-color, SSD (nominal and large-bandwidth), and a combination of four-color with SSD are shown. The adjacent color separation $\delta\lambda$ and the laser bandwidth $\Delta\lambda$ were chosen as appropriate for Nova experiments, namely $\delta\lambda = 0.42$ nm and $\Delta\lambda = 0.25$ nm at 1.06 μm. The ratios $\delta\omega/\omega_0$ and $\Delta\omega/\omega_0$ of frequency separation and bandwidth to laser frequency are assumed to be preserved by frequency tripling or doubling. All the reflectivities shown in Fig. 5 exceed those produced by bremsstrahlung emission or by Thomson scattering from thermal ion acoustic fluctuations. The one-color results are the same as shown in Fig. 4. Below $G = 10$, the effect of beam smoothing is quite dramatic; the reflectivities drop below 10^{-6} for $G \le 6$.

Other $f/4$ simulations have been done with different damping rates, plasma lengths, and laser intensities. At $G \approx 12$, the SSD reflectivities for different simulations vary by five orders of magnitude. The highest reflectivity (1.8%) occurs at the highest intensity, 4×10^{15} W/cm^2, with $L = 515\lambda_0$ and $\upsilon_a/\omega_a = 0.2$; the lowest reflectivity (2×10^{-7}) occurs at the lowest intensity, 1×10^{15} W/cm^2, with $L = 515\lambda_0$ and $\upsilon_a/\omega_a = 0.05$. Increasing the intensity by a factor of two and halving the length to keep G constant also results in higher reflectivity. The reflectivity is increased by an order of magnitude, from 2×10^{-6} to 4×10^{-5}, by doubling the damping υ_a/ω_a from 0.05 to 0.1 and L from $256\lambda_0$ to $515\lambda_0$; it is increased by another order of magnitude to 2×10^{-4} as υ_a/ω_a increases to 0.2 and L to $1030\lambda_0$. Figure 6 shows these results. Both these trends would make sense if the addition of SSD bandwidth increased the effective acoustic wave damping to a value as high as $0.2\omega_a$, so that the effective gain exponent increased with L and/or I. This appears plausible because $\Delta\omega_{SSD}/\omega_0 = 2.5 \times 10^{-4}$, whereas $\upsilon_a/\omega_0 \cong 2(\upsilon_a/\omega_a) \times 10^{-3} = 10^{-4}$ at the lowest damping rate. The light absorption rate $\upsilon = 1/2(n_e/n_c)\upsilon_{ei}$ is even smaller: $\upsilon/\omega_0 \approx 10^{-5}$ for $n_e = 10^{21}$ cm^{-3}, $T_e = 3$ keV, $\lambda_0 = 0.351$ μm, and $Z_{eff} = 5$ (where υ_{ei} is the electron–ion collision frequency).

In Fig. 5, the combination of four-color illumination and 0.025% bandwidth SSD brings the reflectivity below that for any four-color or 0.025% bandwidth SSD simulation at a given gain exponent, as one might expect. Only with gain exponents $G > 20$ is there significant reflectivity; here, the variation of reflectivity with G approaches that calculated for a uniform laser beam. The uniform laser beam reflectivities were calculated with $\upsilon_a/\omega_a = 0.05$ and $L = 515\lambda_0$ and for various intensities up to 4×10^{15} W/cm^2. At the highest gain exponents simulated, $G \approx 50$, all simulations with and without beam smoothing have high reflectivity, $R_{SBS} > 20\%$, for which nonlinear saturation effects other than pump depletion are important. That is, these reflectivities are associated with large-amplitude acoustic waves ($|\delta n_b/n| > 0.5$). A mere reduction in the local magnitude of δn_b without a corresponding limit on the length of plasma over which the waves remain in phase may not produce much reduction in reflectivity. That is, the laser will take longer to deplete but the overall reflectivity will stay nearly constant for large systems.

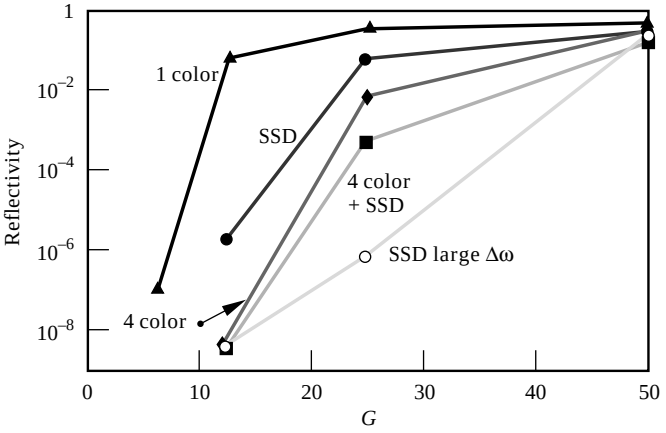

FIGURE 5. $f/4$ SBS reflectivity vs 1-D gain exponent for one-color, SSD, four-color, four-color plus SSD, and SSD with large bandwidth. (50-01-0895-1877pb01)

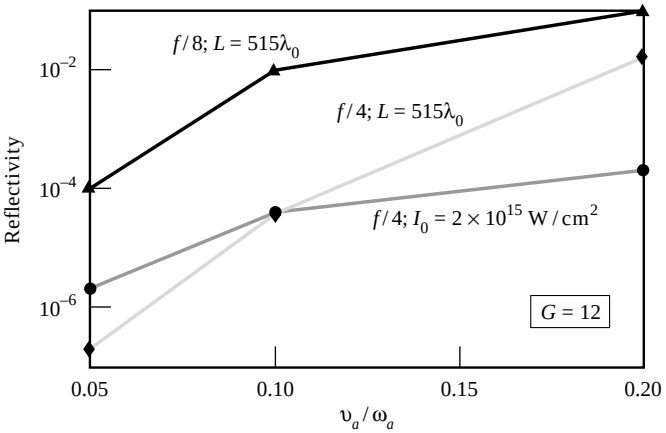

FIGURE 6. SBS reflectivity vs acoustic wave damping rate for a fixed gain exponent $G = 12$ and either a fixed intensity and varying length for $f/4$, a fixed length and varying intensity for $f/4$, or a fixed length and varying intensity for $f/8$. (50-01-0895-1878pb01)

Figure 7 shows the $f/8$ reflectivity calculations for one color, four colors, and four-colors plus SSD. Fewer calculations were carried out for $f/8$ than for $f/4$, but the benefit of the four-color plus SSD combination is also dramatic at $f/8$. Since the speckle length is four times larger than for $f/4$, the smallest length system is $515\lambda_0$, one speckle length. The four-color scheme is not as effective at $f/8$ as at $f/4$ for moderate gain exponents ($G < 20$). The four-color plus SSD reflectivity shows the same trends with intensity and length as the $f/4$ runs for SSD (see Fig. 6).

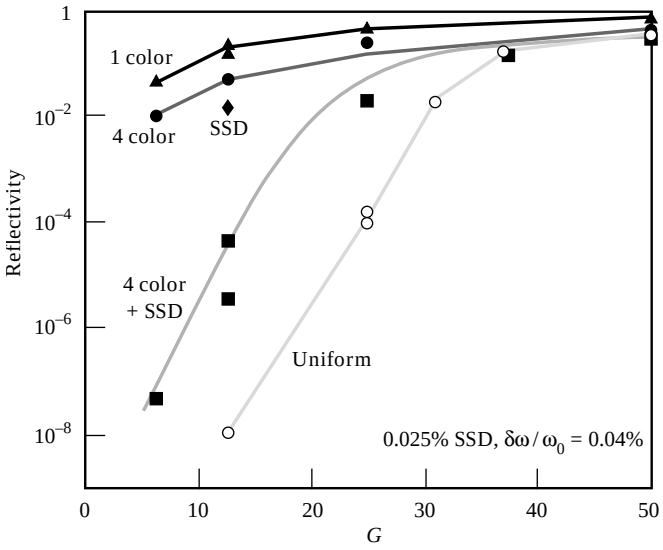

FIGURE 7. $f/8$ SBS reflectivity vs 1-D gain exponent for one-color, four-color, SSD, four-color plus SSD, and uniform laser beams. (50-01-0895-1879pb01)

Conclusions

We have presented three-dimensional calculations of the propagation of laser beams in which the laser light self consistently filaments and Brillouin backscatters. We established that filamentation can be controlled by temporal and spatial beam smoothing for laser and plasma parameters of interest to the proposed NIF. Beam smoothing also reduces the SBBS reflectivity, especially when four-color illumination is combined with SSD. For the gain exponents expected in the NIF,[7] and in experiments designed to reproduce the NIF conditions on Nova,[8] the calculated reflectivities are about 10–20%, whereas the observed reflectivities[20,21] are less than 1–5%. We believe that nonlinear processes, which are not yet modeled in this code, may explain the discrepancy, although other effects that limit the linear gain exponent[22] may also be responsible. A simple nonlinear model[23] (which had some success in modeling disk experiments in which velocity gradients also played a role) did not have much effect on the reflectivity unless the ion wave amplitudes were limited to lower values than typically observed in 1-D particle-in-cell simulations. Recent 2-D simulations have shown much lower ion wave amplitudes than 1-D simulations; we hope to incorporate this amplitude reduction into our code once the effects are understood well enough to reduce to a fluid model.

We also simulated SBBS in plasmas with strong velocity gradients, which limit the reflectivity to small values ($\sim 10^{-4}$). We observed that the reflectivity was produced in one or two spots in which the local reflected light intensity was a significant fraction ($\sim 10^{-2}$) of the local laser intensity. These simulations used the parameters of exploding-foil targets,[24] for which images of the SBBS light were taken at the target plane. These images also showed that only a few spots were responsible for most of the light emission. The reflectivities in the simulations and the experiments were of similar magnitude.

Acknowledgments

We are pleased to acknowledge the benefit of discussions with the Lawrence Livermore National Laboratory plasma experiments group and D. Dubois, J. Kilkenny, W. L. Kruer, J. D. Lindl, L. V. Powers, H. Rose, M. D. Rosen, and S. C. Wilks.

Notes and References

1. Y. Kato, et al., *Phys. Rev. Lett.* 53, 1057 (1984).
2. S. Skupsky, et al., *J. Appl. Phys.* 66, 3456 (1989).
3. R. H. Lehmberg and S. P. Obenschain, *Opt. Commun.* 46, 27 (1983).
4. R. L. Berger, et al., *Phys. Fluids B* 5, 2243 (1993).
5. R. L. Berger, et al., *Phys. Rev. Lett.* 75, 1078 (1995).
6. M. R. Amin, et al., *Phys. Rev. Lett.* 71, 81 (1993); ibid, *Phys. Fluids B* 5, 3748 (1993).
7. C. Labaune, et al., *Phys. Fluids B* 4, 2224 (1992).
8. S. W. Haan, S. M. Pollaine, J. D. Lindl, L. J. Suter, et al., *Phys. Plasmas* 2, 2473 (1995).
9. L. V. Powers, R. L. Berger, D. H. Munro, and B. F. Lasinski, *Phys. Plasmas* 2, 2480 (1995).
10. H. A. Rose and D. F. Dubois, *Phys. Fluids B*, 590 (1993).
11. J. Moody developed a Transmitted Beam Diagnostic (TBD) at Lawrence Livermore National Laboratory to measure the angular distribution of the transmitted laser energy.
12. J. Murray, Lawrence Livermore National Laboratory, Livermore, CA, private communication (1995).
13. D. Pennington, et al., *Tech. Dig.* 8, 161 (1994).
14. S. Dixit, Lawrence Livermore National Laboratory, Livermore, CA, private communication (1995).
15. E. A. Williams, et al., *Phys. Plasmas* 2, 129 (1995).
16. H. A. Rose and D. F. Dubois, *Phys. Rev. Lett.* 72, 2883 (1994).
17. S. L. Wilks, et al., *Phys. Rev. Lett.* 74, 5048 (1995).
18. B. I. Cohen, et al., "Two-Dimensional Hybrid Simulations of Ponderomotively Driven Nonlinear Ion Waves," Lawrence Livermore National Laboratory, Livermore, CA, UCRL-JC-121297 ABS; prepared for the *37th Annual Mtg. of APS Div. of Plasma Phys.*, Louisville, KY, Nov 6–10, 1995.
19. B. Ya Zel'dovich, N. F. Pipiletsky, and V. V. Shkunov, *Principles of Phase Conjugation*, Springer Series in Optical Sciences, T. Tamir, Ed. (Springer, Berlin, 1985), Vol. 42.
20. B. MacGowan, Lawrence Livermore National Laboratory, Livermore, CA, private communication (1995).
21. J. Fernandez, J. A. Cobble, B. H. Failor, W. W. Hsing, et al., *"Dependence of SBS on Laser Intensity, Laser F Number and Ion Species in Hohlraum Plasmas,"* Los Alamos National Laboratory, Los Alamos, NM, LAUR-95-186; submitted to *Phys. Rev. Lett.*
22. B. B. Afeyan, Lawrence Livermore National Laboratory, Livermore, CA, private communication (1995).
23. C. Randall, *1978 Laser Program Annual Report* 1, 3–53, Lawrence Livermore National Laboratory, Livermore, CA, UCRL-50021-78 (1978).
24. C. Labaune, H. A. Baldis, N. Renard, E. Schifano, et al., *Phys. Rev. Lett.* 75(2), 248 (1995).